

# IBM Research Report

## Elastic Strain Relaxation in Free-Standing SiGe/Si Structures

**P. M. Mooney, G. M. Cohen, J. O. Chu, C. E. Murray**

IBM Research Division

Thomas J. Watson Research Center

P.O. Box 218

Yorktown Heights, NY 10598



Research Division

Almaden - Austin - Beijing - Haifa - India - T. J. Watson - Tokyo - Zurich

# Elastic Strain Relaxation in Free-Standing SiGe/Si Structures

P.M. Mooney, G.M. Cohen, J.O. Chu and C.E. Murray

IBM Research Division, T.J. Watson Research Center

Yorktown Heights, NY 10598 USA

## Abstract

We have investigated elastic strain relaxation, i.e. strain relaxation without the introduction of dislocations or other defects, in free-standing SiGe/Si structures. We first fabricated free-standing Si layers supported at a single point by an SiO<sub>2</sub> pedestal and subsequently grew an epitaxial SiGe layer. The measured strain relaxation of the SiGe layer agrees well with that calculated using a force-balance model for strain sharing between the SiGe and strained Si layers. We report strained Si layers with biaxial tensile strain equal to 0.007 and 0.012.

Many semiconductor devices utilize strained layers to enhance device performance. One important example is strained Si MOSFETs in which the active region is a Si layer under tensile strain [1]. In typical device structures, the strained Si layer is a pseudomorphic epitaxial layer grown on a thick strain-relaxed graded SiGe buffer layer on Si(001) [1]. Epitaxial SiGe layers on Si(001) typically relax by the introduction of misfit dislocations near the SiGe/Si interface and much work has been done to achieve the desired degree of strain relaxation with a sufficiently low threading dislocation density for device applications [2]. Reported values for threading dislocation densities in graded SiGe buffer layers range from  $10^5$  to  $10^8$   $\text{cm}^{-2}$  [2]. The electron mobility in strained Si field-effect transistors was shown to decrease when the threading dislocation density  $>3 \times 10^8$   $\text{cm}^{-2}$  [3]. However, it is not yet known how low the threading density must be to avoid problems with various device processes and achieve the very high device yield and reliability needed for ultra-large-scale integration applications.

So-called “compliant substrates” are a possible way to reduce defect densities in strained Si structures [4,5]. The ideal compliant substrate is air, as was demonstrated by light emission at 1.34  $\mu\text{m}$  from an  $\text{In}_{0.4}\text{Ga}_{0.6}\text{As}$  quantum well grown on free-standing  $\text{In}_{0.05}\text{Ga}_{0.95}\text{As}$  indicating that the cladding layers are unstrained [6]. Here we report elastic strain relaxation, i.e., strain relaxation of a SiGe layer without the introduction of dislocations or other defects, in free-standing SiGe/Si structures. We find that the degree of strain relaxation of the SiGe layer agrees well with that calculated using a force-balance model for strain sharing, or strain partitioning, between the SiGe and Si layers.

The free-standing structures investigated were fabricated from silicon-on-insulator (SOI) substrates made by bonding a thin Si layer onto a 1  $\mu\text{m}$ -thick thermally grown  $\text{SiO}_2$  film on a Si(001) substrate. The SOI film was then further thinned by thermal oxidation to about 30 nm and patterned into an array of 5  $\mu\text{m}$  x 5  $\mu\text{m}$  squares by conventional photolithography and reactive ion etching (RIE). Large un-patterned areas of the SOI wafer and exposed bulk Si areas were included as reference regions. The patterned SOI layer was then undercut to form a free-standing Si film by selectively etching the  $\text{SiO}_2$  layer. The resulting structure resembles a mushroom in cross section with an  $\text{SiO}_2$  pedestal that supports the Si slab at a single contact point at the center of the slab. The diameter of the pedestal is typically 0.7  $\mu\text{m}$ . Finally, epitaxial layers of  $\text{Si}_{0.81}\text{Ge}_{0.19}$  or  $\text{Si}_{0.68}\text{Ge}_{0.32}$  were grown on the wafer by ultra-high vacuum chemical vapor deposition [7]. The thickness of the  $\text{Si}_{0.81}\text{Ge}_{0.19}$  was less than or equal to the critical thickness for plastic strain relaxation of a blanket film, whereas the thickness of the  $\text{Si}_{0.68}\text{Ge}_{0.32}$  layer exceeds the critical thickness for plastic strain relaxation. On the patterned regions the SiGe grows on all the exposed surfaces of the free-standing Si slab as well as on the exposed Si substrate surrounding the free-standing structures. Fig. 1 shows an SEM image of the final structure. The faceting of the SiGe layer clearly indicates single-crystal epitaxial growth. Closer inspection shows a very thin polycrystalline SiGe layer on the sides of the  $\text{SiO}_2$  pedestal. Additional SEM images and further details about the fabrication process can be found in Ref. 8.

X-ray measurements were performed using a Philips XPert Pro diffraction system equipped with a hybrid incident beam monochromator consisting of a mirror and a four-

bounce Ge crystal that gives a 1mm x 10mm incident Cu-K $_{\alpha}$  beam ( $\lambda = 1.542 \text{ \AA}$ ) with a divergence of  $0.007^{\circ}$ . Triple-axis measurements were done using a three-bounce Ge analyzer crystal in front of the detector.  $\omega$  is the angle between the incident beam and the sample surface and  $2\theta$  is the angle between the detector (diffracted beam) and the incident beam, i.e. it is twice the Bragg angle  $\theta_B$ .

Figs. 2(a) and 2(b) are triple-axis diffraction maps of the blanket SOI and the patterned areas respectively of a Si $_{0.81}$ Ge $_{0.19}$ /Si sample having layer thickness ratio 8.8. Note that there is an offset in  $\omega$  between the diffraction peaks from the SiGe and SOI layers and the Si substrate (Fig. 2(a)), indicating a slight misalignment between the (001) lattice planes of the substrate and those of the bonded SOI layer [9]. This tilt angle aids the measurement of the thin SOI layer in the presence of the strong substrate peak. The SiGe and Si peaks from the patterned SOI region are both shifted to higher Bragg angle ( $\theta_B$ ) compared to those of the un-patterned SOI region, indicating different lattice parameters in the two regions. The degree of strain relaxation in the free-standing SiGe layers is determined from the change in the Bragg angle compared to that of the SiGe on bulk Si surrounding the free-standing structures and corresponds to relaxation of 93% of the mismatch strain in this sample. We also find that the angular separation between the Si and SiGe peaks is the same on all regions of the sample: the SOI reference, the Si substrate reference, the Si substrate surrounding the free-standing structure and on the free-standing structure, indicating that strain relaxation in the free-standing structures has occurred elastically, i.e. without the formation of misfit dislocations. Elastic strain relaxation was confirmed by atomic force microscopy (AFM) measurements that show

that the usual cross hatch pattern seen on plastically relaxed SiGe layers is not present on the relaxed free-standing SiGe/Si structures [8]. During epitaxial growth, the strain in the SiGe layer is transferred to the free-standing SOI layer, thus causing it to be under biaxial tensile strain, as seen from the shift of  $\theta_B$  of the free-standing SOI film (Fig. 2).

Figs. 3(a) and 3(b) show individual triple-axis scans taken from the SiGe/SOI layers in the blanket and patterned areas respectively of  $\text{Si}_{0.81}\text{Ge}_{0.19}/\text{Si}$  sample having layer thickness ratio 0.8. The presence of strong thickness fringes in these scans confirms that the SiGe layer is pseudomorphic to the Si layer, i.e., that there is a negligible dislocation density at the SiGe/Si interface in both regions of the sample. Assuming that negligible strain relaxation occurs in the blanket reference areas, simulations of the scans from the blanket SOI region using the Philips Epitaxy software yield the alloy composition of SiGe layers from the angular separation of the SiGe and Si layer peaks and the thickness of both layers from the spacing of the thickness fringes. In this case the model used for the simulation consists of two layers, the SOI layer and the epitaxial SiGe layer. We can extract the thickness of both the SOI and the SiGe layers from the simulations of the data from the free-standing structures. Here the model consists of three layers, corresponding to the SiGe layers on the top and bottom of the Si slab, as shown in Fig. 4. We find that the SiGe layer grown on free-standing Si is 10-20% thinner than on the blanket SOI layer, presumably due to the relatively poor thermal contact between the free-standing Si and the Si substrate. The mismatch strain between the SiGe layer and the free-standing Si is essentially the same as that on the un-patterned SOI and exposed Si substrate, as seen from the angular separation of their diffraction peaks indicating a

negligible change in the alloy composition. As was also seen in Fig. 2, the diffraction peaks for both the SiGe and the SOI layers are shifted to higher Bragg angles on the patterned areas. The shift in the Bragg angle of the SiGe layer indicates that 46% of the mismatch strain is transferred to the Si layer in this sample.

The free-standing SiGe/Si structure can be described by a linear elastic model in which a force balance between the Si and SiGe layers of the composite is generated by their lattice mismatch. Because of the vertical symmetry of the structure, bending can be neglected, as confirmed by the absence of broadening of the free-standing SiGe layer peak along the  $\omega$  axis in Fig. 3. For pseudomorphic SiGe and Si layers with no misfit dislocations present, the Si layer is in a state of isotropic biaxial tension due to a force per unit length  $P$  whereas the SiGe layers are in isotropic biaxial compression due to the corresponding force per unit length  $-P$ , as shown in Fig. 4. For a planar stress ( $\sigma_{31}=\sigma_{32}=\sigma_{33}=0$ ) and assuming that the effects of the free edges and the supporting pedestal have a negligible contribution to the average strain in the Si and SiGe layers, the only non-zero components of the stress tensor are the in-plane normal stresses ( $\sigma_{11}=\sigma_{22}=\sigma$ ). Because of the force balance between the Si and SiGe layers, we can relate their in-plane stress to  $P$ , which stretches the Si and compresses the SiGe:  $\sigma_{\text{Si}}=P/t_{\text{Si}}$  and  $\sigma_{\text{SiGe}}=-P/t_{\text{SiGe}}$ , where  $t_{\text{Si}}$  and  $t_{\text{SiGe}}$  are the total thickness of the Si and SiGe layers, respectively. It is straightforward to preserve the cubic symmetry of the Si and SiGe features in the expressions for the in-plane strains:  $\epsilon_{\text{Si}}=[S_{11}(\text{Si})+S_{12}(\text{Si})]P/t_{\text{Si}}$  and  $\epsilon_{\text{SiGe}}=-[S_{11}(\text{SiGe})+S_{12}(\text{SiGe})]P/t_{\text{SiGe}}$ , where  $S_{11}$  and  $S_{12}$  are the crystal compliance values for the Si and SiGe films.

The assumption of a coherent interface between the Si and SiGe layers requires that the difference in the in-plane strain values between the Si and SiGe is due to the lattice mismatch,  $\epsilon_{\text{Si}} = \epsilon_{\text{SiGe}} + \Delta\epsilon$ . Combining the above equations and solving for the force per unit length,  $P$ , we arrive at an expression for the in-plane strain as a function of the lattice mismatch and the elastic properties of the Si and SiGe,  $\epsilon_{\text{Si}} = \Delta\epsilon / [1 + t_{\text{Si}}M_{\text{Si}}/t_{\text{SiGe}}M_{\text{SiGe}}]$  and  $\epsilon_{\text{SiGe}} = -\Delta\epsilon / [1 + t_{\text{SiGe}}M_{\text{SiGe}}/t_{\text{Si}}M_{\text{Si}}]$ , where  $M = 1/(S_{11} + S_{12})$  represents the biaxial moduli of the Si and SiGe. For elastically isotropic materials,  $M = E/(1-\nu)$ , where  $\nu$  is the Poisson ratio, which produces the traditional expression for the in-plane strain [10].

In Fig. 5 the strain relaxation in the SiGe layer, expressed as a fraction of the mismatch strain, is plotted against the ratio of the layer thicknesses,  $t_{\text{SiGe}}/t_{\text{Si}}$ , calculated using the force balance model along with the experimental values determined from the x-ray data. The agreement between the model and the experiment is excellent, indicating that the free-standing structures are indeed elastically relaxed, *even when the SiGe layer thickness exceeds the critical thickness for plastic strain relaxation of a blanket film*. Note that for  $t_{\text{SiGe}}/t_{\text{Si}} = 9$ , 90% of the strain has been transferred to the Si layer and that further increases in the thickness ratio will not significantly increase the strain in the Si layer. This results in a Si layer under biaxial tensile strain of 0.007 for  $\text{Si}_{0.81}\text{Ge}_{0.19}$  and of 0.012 for  $\text{Si}_{0.68}\text{Ge}_{0.32}$ .

In summary we have demonstrated elastically strained Si layers on free-standing SiGe/Si structures. Because strain relaxation in these structures is elastic, misfit dislocations are not introduced to relieve the strain in the SiGe layer. Thus defect



densities are many orders of magnitude lower than in the best quality strain-relaxed SiGe buffer layers currently used for strained Si MOSFETs.

## References

1. K. Rim, J.L. Hoyt, J.F. Gibbons, IEEE Trans. Electron Devices **47**, 1406 (2000).
2. P.M. Mooney, Materials Science and Engineering Reports R17, 105 (1996); and references therein.
3. K. Ismail, J. Vac. Soc. Technol. B 14, 2776 (1996).
4. H. Yin, R. Huang, K.D. Hobart, Z. Suo, T.S. Kuan, C.K. Inoki, S.R. Shieh, T.S. Duffy, F.J. Kim and J.C. Strum, J. Appl. Phys. **19**, 9716 (2002).
5. H. Yin, K.D. Hobart, F.J. Kub, S.R. Shieh, T.S. Duffy and J.C. Sturm, Appl. Phys. Lett. **82**, 3858 (2003).
6. A.M. Jones, J.L. Jewel, J.C. Mabon, E.E. Reuter, S.G. Bishop, S.D. Roh and J.J. Coleman, Appl. Phys. Lett. **74**, 1000 (1999).
7. B.S. Meyerson, Appl. Phys. Lett. **48**, 797 (1986).
8. G.M. Cohen, P.M. Mooney and J.O. Chu, Mat. Res. Soc. Symp. Proc. **768**, 9 (2003).
9. G.M. Cohen, P.M. Mooney, E.C. Jones, K.K. Chan, P.M. Solomon and H-S. P. Wong, Appl. Phys. Lett. **75**, 787 (1999).
10. L.D. Landau and E.M. Lifshitz, *Theory of Elasticity, Course of Theoretical Physics*, Vol. 7 (Pergamon, London, 1959).

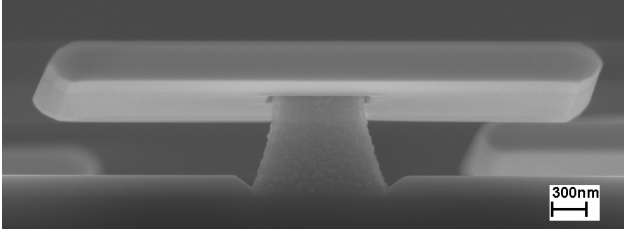


Figure 1. SEM image of a free-standing  $\text{Si}_{0.81}\text{Ge}_{0.19}/\text{Si}/\text{Si}_{0.81}\text{Ge}_{0.19}$  structure supported by an  $\text{SiO}_2$  pedestal. The scale bar is 300nm.

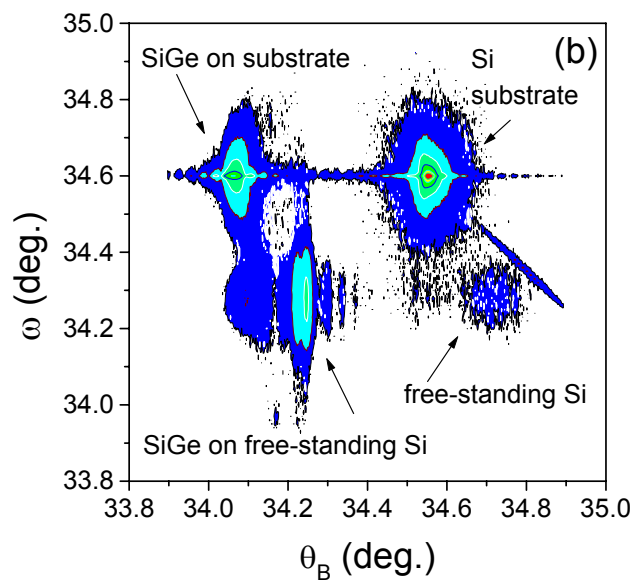
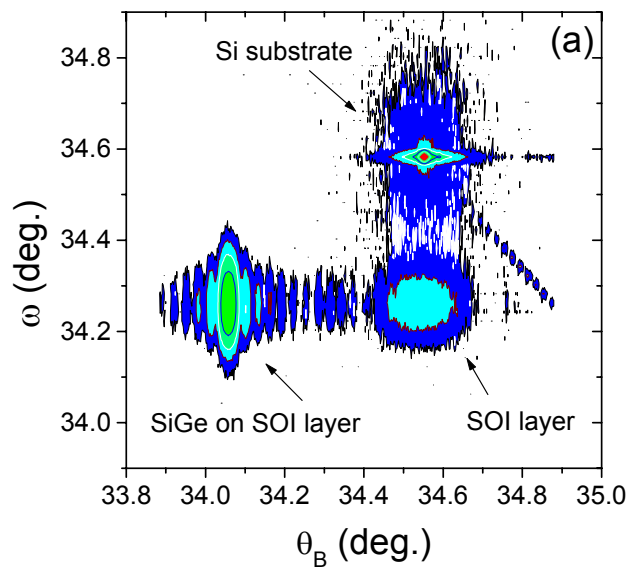


Figure 2. Triple-axis x-ray maps of (a) the SOI reference area and (b) the area with free-standing  $\text{Si}_{0.81}\text{Ge}_{0.19}/\text{Si}/\text{Si}_{0.81}\text{Ge}_{0.19}$  structures.

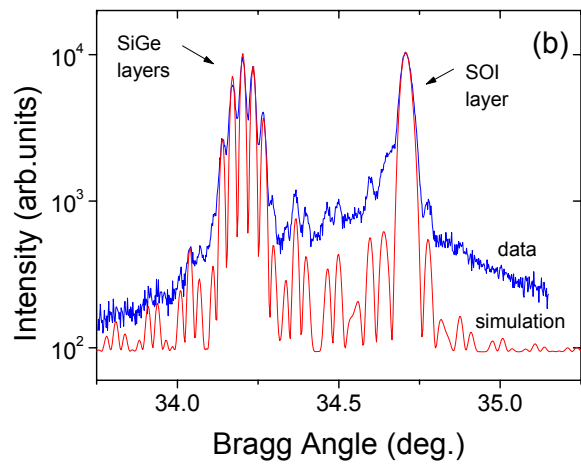
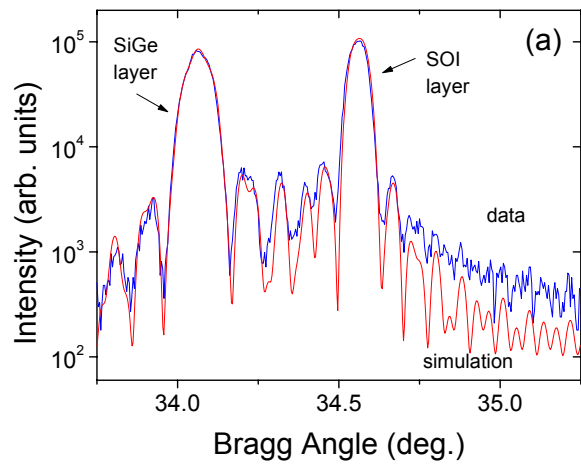


Figure 3. Triple-axis scans of (a) the  $\text{Si}_{0.81}\text{Ge}_{0.19}$  and SOI layers on the reference area and (b) the free-standing structures.

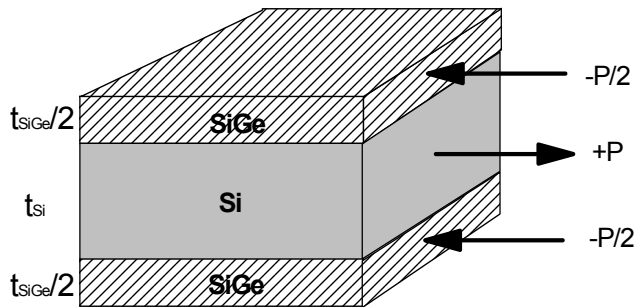


Figure 4. Schematic diagram of the free-standing SiGe/Si/SiGe structures used for the model and the x-ray data analysis.

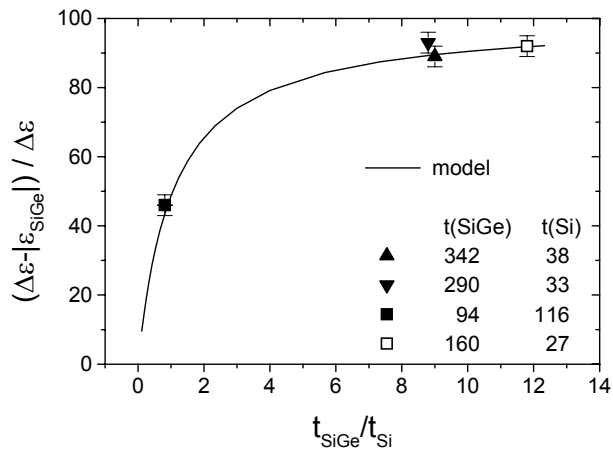


Figure 5. Plot of SiGe strain relaxation from the model with experimental data. Solid symbols are  $\text{Si}_{0.81}\text{Ge}_{0.19}$  and open symbols are  $\text{Si}_{0.68}\text{Ge}_{0.32}$ . The layer thickness,  $t$ , is measured in nm.